4'-O-methylbavachalcone inhibits succinate induced cardiomyocyte hypertrophy via the NFATc4 pathway

HAN SUN, GUANGHAO ZHU, SHUANG LING, JUN LIU and JIN-WEN XU

Institute of Interdisciplinary Medical Science, Shanghai University of Traditional Chinese Medicine, Pudong New Area, Shanghai 201203, P.R. China

Received September 22, 2022; Accepted February 7, 2023

DOI: 10.3892/etm.2023.11871

Abstract. Pathological cardiac hypertrophy is an independent risk factor for complications such as arrhythmia, myocardial infarction, sudden mortality and heart failure. Succinate, an intermediate product of the Krebs cycle, is released into the bloodstream by cells; its levels increase with exacerbations of hypertension, myocardial and other tissue damage and metabolic disease. Succinate may also be involved in several metabolic pathways and mediates numerous pathological effects through its receptor, succinate receptor 1 (SUCNR1; previously known as GPR91). Succinate-induced activation of SUCNR1 has been reported to be related to cardiac hypertrophy, making SUCNR1 a potential target for treating cardiac hypertrophy. Traditional Chinese medicine (TCM) and its active ingredients have served important roles in improving cardiac functions and treating heart failure. The present study investigated whether 4'-O-methylbavachadone (MeBavaC), an active ingredient of the herbal remedy Fructus Psoraleae, which is often used in TCM and has protective effect on myocardial injury and hypertrophy induced by adriamycin, ischemia-reperfusion and sepsis, could ameliorate succinate-induced cardiomyocyte hypertrophy by inhibiting the NFATc4 pathway. Using immunofluorescence staining, reverse transcription-quantitative PCR, western blotting and molecular docking analysis, it was determined that succinate activated the calcineurin/NFATc4 and ERK1/2 pathways to promote cardiomyocyte hypertrophy. MeBavaC inhibited cardiomyocyte hypertrophy, nuclear translocation of NFATc4 and ERK1/2 signaling activation in succinate-induced cardiomyocytes. Molecular docking analysis revealed that MeBavaC interacts with SUCNR1 to form a relatively stable binding and inhibits the succinate-SUCNR1 interaction. The results demonstrated that MeBavaC suppressed cardiomyocyte hypertrophy by blocking SUCNR1 receptor activity and inhibiting NFATc4 and ERK1/2 signaling, which will contribute to the preclinical development of this compound.

Correspondence to: Professor Jin-Wen Xu or Dr Jun Liu, Institute of Interdisciplinary Medical Science, Shanghai University of Traditional Chinese Medicine, 1200 Cailun Road, Pudong New Area, Shanghai 201203, P.R. China
E-mail: jwxu1001@163.com
E-mail: junliu1995@163.com

Abbreviations: Ang II, angiotensin II; ERK1/2, extracellular signal-regulated kinases 1/2; JNK, c-Jun N-terminal kinases; MAPK, mitogen-activated protein kinases; MeBavaC, 4'-O-methylbavachalcone; MTT, 3-[4,5-dimethylthiazol-2-yl]-2,5 diphenyl tetrazolium bromide; NFATc, nuclear factor activated T cell; PBS, phosphate-buffered saline; PLCβ, Phospholipase C beta; SUCNR1/GPR91, succinate receptor 1; TAC, tricarboxylic acid; TCM, Traditional Chinese Medicine

Key words: succinate, succinate receptor 1, cardiomyocyte hypertrophy, nuclear factor activated T cell, 4'-O-methylbavachalcone

Introduction

Pathological cardiac hypertrophy is an independent risk factor for arrhythmia, myocardial infarction, sudden death and heart failure. Concentric ventricular hypertrophy results in systolic or diastolic dysfunction and can be caused by chronic hypertension, aortic stenosis, myocardial infarction, hereditary cardiomyopathy, obesity and diabetes (1-3). Pathological cardiac hypertrophy is characterized by numerous decompensations, such as cardiomyocyte death, fibrosis, Ca^{2+}-regulated protein dysregulation, mitochondrial dysfunction, metabolic reprogramming, reactivation of fetal gene expression, altered sarcomere structure and insufficient angiogenesis leading to microvascular sparseness (4-8).

Calcineurin is a cytoplasmic Ca^{2+}/calmodulin-dependent protein phosphatase that contributes to pathological cardiac hypertrophy. The calcineurin/nuclear factor-activated T-cell (NFATc) pathway affects cardiac structure under pathological conditions and serves a role in cardiac hypertrophy (9,10). In the adult heart, NFATc activity is continuously upregulated during pathological cardiac hypertrophy caused by pressure overload or hypertension and is more pronounced after myocardial infarction-induced heart failure (11,12). NFATc4 is required for calcineurin-mediated cardiomyocyte hypertrophy (13,14). Angiotensin II (Ang II) or phenylephrine can activate calcineurin/NFATc4 to promote cardiomyocyte hypertrophy (15).

The tricarboxylic acid (TAC) cycle in the mitochondrial matrix is considered a core process in cellular metabolism and energy balance (16-18). Succinate is an intermediate of

this cycle and its concentrations are significantly increased in hypertensive, obese and diabetic animal models (19). It is also the only metabolite whose levels are significantly increased in the coronary sinus of patients with ST-segment elevation myocardial infarction (STEMI) (20). Succinate produces broad pathophysiological effects by binding to the G-protein-coupled receptor 91 (GPR91)/Succinate receptor 1 (SUCNR1). SUCNR1 is expressed in the kidney, liver, heart, retinal cells and other tissues and is involved in regulating blood pressure, inhibiting lipolysis of white fat, forming retinal blood vessels, promoting cardiac hypertrophy and activating hepatic stellate cells (21,22). In a pulmonary arterial hypertension model of pressure overload-induced right ventricular hypertrophy in Sprague-Dawley rats, succinate treatment further aggravated right ventricular hypertrophy, upregulated the right ventricular hypertrophy-related gene ANP and activated PI3K/Akt axis signaling (23). Succinate was found to cause cardiac hypertrophy in SUCNR1-null mice in a SUCNR1-dependent manner. Activation of SUCNR1 triggers signals of cardiac hypertrophy such as phosphorylation of extracellular signal-regulated kinases 1/2 (ERK1/2) and expression of calmodulin-dependent protein kinase II delta (CaMKIIδ) (24).

Fructus Psoraleae (the dried fruits of *Psoralea corylifolia L.*) is a common herb in traditional Chinese medicine (TCM) that has been included in Chinese Pharmacopoeia records (25). According to the theory of TCM, Fructus Psoraleae has the effect of warming and tonifying the kidney-Yang. It is widely used in the treatment of coronary artery disease, osteoporosis, vitiligo and psoriasis. Psoralea mainly contains coumarin, terpene phenol and prenylflavonoids, which are the material basis of drug treatment. Our team has summarized the pharmacological effects of five major psoralea prenylflavonoids, which have anti-inflammatory, cardiovascular protective, neuroprotective and antiosteoporosis effects (26). 4'-O-methylbavachalcone (MeBavaC) (Fig. 1B) is a prenylflavonoid that is abundantly present in Fructus Psoraleae (27). Few pharmacological studies have been conducted on MeBavaC; the only known report on the subject indicated that MeBavaC inhibits SARS-CoV papain-like protease PLpro (28). The present study investigated whether MeBavaC can ameliorate succinate-induced cardiomyocyte hypertrophy by inhibiting the calcineurin/NFATc4 pathway. The results revealed that succinate activated the calcineurin/NFATc4 and ERK1/2 pathways to promote cardiomyocyte hypertrophy and that MeBavaC treatment inhibited succinate-induced cardiomyocyte hypertrophy and related signaling; In addition, molecular docking analysis indicated that MeBavaC interacted with SUCNR1 to form a relatively stable binding and produced a certain inhibitory effect.

Materials and methods

Reagents and antibodies. Sodium succinate and Dulbecco's modified Eagle's medium (High Glucose) were purchased from MilliporeSigma. Fetal bovine serum was obtained from Gibco; Thermo Fisher Scientific, Inc. Penicillin-streptomycin solution, trypsin cell digestion solution (containing 0.25% trypsin and phenol red), cDNA first-strand synthesis kit (cat. no. D7178L), RIPA lysis solution (cat. no. P0013B) and BCA protein concentration assay kit (cat. no. P0012) were purchased from Beyotime Institute of Biotechnology. Dimethyl sulfoxide, Triton X-100, paraformaldehyde and anhydrous ethanol were purchased from Shanghai Titan Scientific Co., Ltd. Trichloromethane and isopropanol were purchased from Sinopharm Chemical Reagent Co., Ltd. Tetramethylrhodamine (TRITC)-phalloidin (cat. no. MX4405-300T) was purchased from Shanghai Maokang Biotechnology Co., Ltd. Power SYBR Green PCR master mix (cat. no. 4367659) was purchased from Thermo Fisher Scientific, Inc. Anti-GAPDH (cat. no. 2118), anti-phospho-p38 MAPK (cat. no. 4511), anti-phospho-SAPK/JNK (cat. no. 4668), anti-SAPK/JNK (cat. no. 9252), anti-phospho-p44/42 MAPK (cat. no. 4370), anti-p44/42 MAPK (cat. no. 4695), anti-NFAT3/NFATc4 (23E6) rabbit mAb (cat. no. 2183) and antimouse IgG (cat. no. 7076) were purchased from Cell Signaling Technology, Inc. Anti-p38α/β (sc-7149) was obtained from Santa Cruz Biotechnology, Inc. Donkey anti-rabbit IgG H&L (Alexa Fluor 488; cat. no. ab150073) was obtained from Abcam. Antirabbit IgG (cat. no. MR-R100) was purchased from Shanghai Mingrui Biotech Co., Ltd. PD98059 (cat. no. S1177), SP600125 (cat. no. S1640) and SB203580 (cat. no. S1076) were purchased from Selleck Chemicals. VIVIT (cat. no. HY-P1026) was obtained from MedChemExpress. Cyclosporin A (cat. no. A600352-0001) was purchased from Sangon Biotech Co., Ltd.

Cell culture. H9c2 cardiomyocytes (American Type Culture Collection) were cultured in DMEM containing 10% FBS supplemented with antibiotics (100 U/ml penicillin G and 100 μg/ml streptomycin sulfate) at 37˚C in a humidified atmosphere of 5% CO_2.

MTT assay. H9c2 cells were seeded into a 96-well plate (5,000 cells/well) and cultured overnight in a 37˚C and 5% CO_2 cell incubator. On the second day, sodium succinate or MeBavaC with different final concentrations (diluted with serum- and antibiotic-free H-DMEM medium) was added, whereas for the control group, the same amount of H-DMEM medium was added. Then, six parallel wells were set up for each group. After 48 h, 10 μl of MTT solution [5 mg/ml in phosphate-buffered saline (PBS)] was added to each well and incubated for 4 h at 37˚C and 5% CO_2. Next, 150 μl of DMSO solution was mixed with the cell-MTT suspension and the formazan crystals were fully dissolved by shaking on a constant temperature microtiter plate with a fast shaker for 10 min. The OD value of each well was detected using a Varioskan Flash microplate spectrophotometer (Thermo Fisher Scientific, Inc.) at 570 nm.

Cell size analysis. The cell surface area was determined by staining the cells with TRITC-phalloidin. Briefly, the H9C2 cells were seeded at a density of 10,000 cells/plate in a 12-well plate. On the basis of the principle that phalloidin can combine with actin (29), when the confluence of H9c2 cells reached 50%, TRITC-phalloidin staining was performed to observe cardiomyocyte hypertrophy induced by succinate. Phalloidin staining of F-actin as a marker for measuring cell surface area has been used in numerous cell experiments (30,31). The cells were incubated with or without MeBavaC and then treated with

1 mM sodium succinate for 0-48 h. They were then washed with PBS and fixed with 4% formaldehyde solution for 10 min at room temperature, followed by washing twice with PBS. The cells were then treated with 0.5% Triton X-100 at room temperature for 5 min to increase permeability then washed twice with PBS. Finally, the cells were stained with 100 nM TRITC-Phallodin staining solution for 30 min in the dark at room temperature with gently shaking. The cells were washed twice with PBS, which was followed by staining with DAPI for ~30 sec at room temperature. After washing, fluorescence microscopy images were recorded separately at excitation/emission wavelengths (Ex/Em=546/575 nm for TRITC and Ex/Em=364/454 nm for DAPI). A total of five images were taken from each plate of cells from different areas (each group n=3; counting 50 cells). Under an Olympus IX71 microscope (Olympus Corporation), the 'Count and Measure' facility in the imaging software CellSens 1.14 (Olympus Corporation) was used, the cell regions of interest were selected and defined, automatic image size measurement was implemented and the area test parameters were derived for statistical analysis.

Immunofluorescence. Following treatment, the H9c2 cells were fixed in 4% paraformaldehyde for 10 min at room temperature and then permeabilized with 1% Triton X-100 for 10 min at room temperature. After blocking with 5% bovine serum albumin (MilliporeSigma), the H9c2 cells were incubated with the anti-NFATc4 overnight at 4˚C in a humidified chamber. This was followed by incubation with donkey antirabbit IgG H&L (Alexa Fluor® 488) for 2 h at 37˚C. After washing, images were taken with an immunofluorescence microscope (Olympus IX71; Olympus Corporation).

Reverse transcription-quantitative (RT-q) PCR. According to the manufacturer's user manuals, total RNA was extracted from ~5x10^6 cultured cardiomyocytes per sample with NucleoSpin RNA Plus kit (Takara Bio, Inc.) and cDNA was synthesized using the BeyoR III cDNA Synthesis kit (Beyotime Institute of Biotechnology). Gene expression analysis was performed on an ABI 7500 Fast real-time PCR system using the Power SYBR Green PCR master mix according to the manufacturer's instructions (Thermo Fisher Scientific, Inc.). The primer sequences (synthesized by Sangon Biotech Co., Ltd.) were: rat GAPDH: forward primer 5'-GATCCCGCTAACATC AAATG-3', reverse primer 5'-GAGGGAGTTGTCATATTT CTC-3'; rat α-actinin: forward primer 5'-AGAAGAGATCGT GGATGGCAATGC-3', reverse forward primer 5'-GATGTC TTGGATGGCGAACCTGAG-3'; rat GATA4: forward primer 5'-CCTCCTTCTCTACCTGCCTGTCC-3'; and reverse primer 5'-TGTCTTGAAGCCTCGGTCCCTAC-3'. Gene expression was normalized to the reference gene GAPDH. The reaction conditions were: Denaturation (95˚C for 10 min), annealing (60˚C for 1 min) and extension (95˚C for 15 sec) for 40 cycles. Three independent experiments were conducted. PCR results were calculated using the $2^{-\Delta\Delta Cq}$ method and statistically analyzed (32).

Western blotting analysis. The cultured cells were washed twice with cold PBS containing PMSF (1 mM), NaF (2 mM) and Na_3VO_4 (2 mM) and then lysed with 100 μl of RIPA lysis buffer containing PMSF, NaF and Na_3VO_4 at the same final concentration. The cells at the bottom of the dish were collected with a scraper into a 1.5 ml microcentrifuge tubes, lysed on ice for 30 min and then centrifuged at 13,400 x g in a microcentrifuge for 15 min at 4˚C. The supernatant was taken into new prechilled 1.5 ml microcentrifuge tubes and employed for measuring the protein concentration at 562 nm by using a bicinchoninic acid protein assay kit. The protein samples were adjusted to a uniform concentration with SDS-PAGE protein loading buffer (5X) and PBS and then denatured in a water bath at 95˚C for 10 min. Protein (30 μg) was separated by performing 10% SDS-PAGE and transferred to nitrocellulose membranes (Pall Filter Beijing Co. Ltd.). The membranes were blocked at room temperature for 2 h with 5% non-fat dried milk in a buffer containing 140 mmol/l NaCl, 20 mmol/l Tris-HCl (pH 7.5) and 0.1% Tween-20 and incubated overnight at 4˚C with the primary antibodies (dilution ratio: 1:1,000). Finally, the membranes were incubated for 2 h with horseradish peroxidase-conjugated mouse monoclonal antibody (1:2,000) at room temperature with gentle shaking. The PVDF membrane was immersed in ECL working solution (Sangon Biotech Co., Ltd.) and incubated in the dark for 1 min. The membrane was placed in a chemiluminescence developer (Tanon Science and Technology Co., Ltd.) for gradient exposure and the images was captured with the Tanon-5200 Multi chemiluminescent imaging system (Tanon Science and Technology Co., Ltd.), which uses the Sony ICX694 sensor CCD chip. Quantitative analysis of band density was performed using Quantity One (version 25.0) software from Bio-Rad Laboratories, Inc.

Molecular docking simulations. Molecular docking simulations were performed to analyze the inhibitory mechanism of compounds against SUCNR1. Due to the absence of a crystal structure of human SUCNR1, the structure of a rat SUCNR1 (PDB Code: 6IBB) was acquired from the Protein Data Bank (https://www.rcsb.org) and was used as a receptor (33,34). Graphical user interface AutoDock (https://ccsb.scripps.edu/) Tools 1.5.6 software was used to format coordinate files of SUCNR1 and compounds by adding polar hydrogens, deriving Kollman charges and setting AutoDock 4 type of atoms. The SUCNR1 docking site was placed at the orthosteric site described in previous studies (34,35). The grid box was settled to encircle the orthosteric site and AutoDock Vina (1.1.2) was used as the docking and scoring program. Further analyses of the SUCNR1-inhibitor interactions based on the docking and scoring results were aided by BIOVIA Discovery Studio Visualizer (Dassault Systemes).

Statistical analysis. GraphPad Prism 7 software (Dotmatics) was used for data analysis and statistics and the data were expressed as means ± standard deviations. Comparisons between groups were analyzed using one-way analysis of variance followed by Dunnett's multiple comparison test. $P<0.05$ was considered to indicate a statistically significant difference.

Results

Succinate induces cardiomyocyte hypertrophy and activates nuclear translocation of NFATc4. First, MTT assay was used to evaluate the effects of sodium succinate and MeBavaC on the survival of H9C2 cardiomyocytes. Sodium succinate was

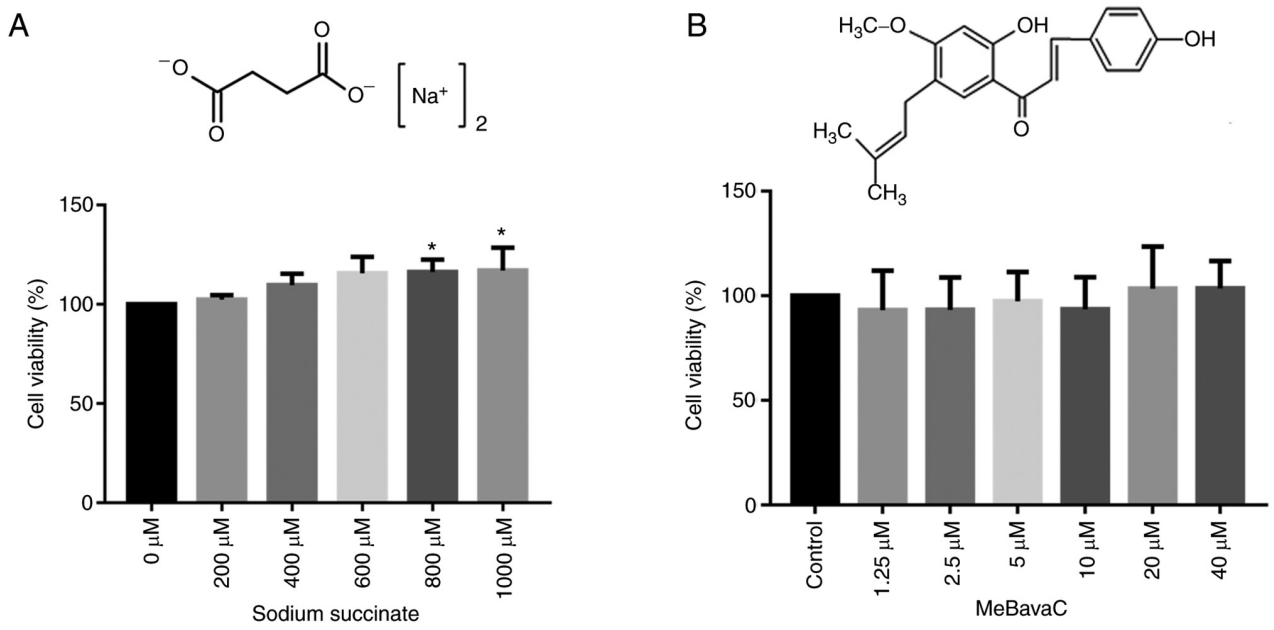

Figure 1. Effects of sodium succinate and MeBavaC on the viability of H9c2 cardiomyocytes. After H9c2 cells were treated with the indicated concentrations of (A) sodium succinate or (B) MeBavaC for 48 h, an MTT test was performed (six wells per test; n=3 tests). Comparisons between the groups were analyzed completed using Dunnett's multiple comparison test after one-way ANOVA. Data are expressed as mean ± standard deviation. *P<0.05 vs. 0 μM group. MeBavaC, 4'-O-methylbavachalcone.

dissolved in DMEM medium and MeBavaC was dissolved in DMSO as a stock solution and diluted with the medium to the final concentration. The final concentration of DMSO was <0.1%, which ensured it was safe for the cells. As presented in Fig. 1A, no cytotoxicity was detected in the H9C2 cells, indicating that the concentrations of sodium succinate within 1,000 μM and stimulation for 48 h were safe (six wells per test, n=3 tests). In addition, the effects of 1, 2, 5, 10, 25 and 50 mM sodium succinate on the H9C2 cardiomyocytes was measured and no toxicity found (data not shown). When the cardiomyocytes were treated with 800 and 1,000 μM of sodium succinate, a slight increase in MTT was observed (116.4±5.5 and 117.1±5.5, respectively). The effect of MeBavaC within 40 μM on H9C2 cells was also tested and no cytotoxicity was discovered (six wells per test, n=3 tests, Fig. 1B). Given that no cytotoxicity was noted with 1 mM sodium succinate (Fig. 1A) and that this concentration has also been used in a number of studies (24,36), 1 mM sodium succinate was used in all subsequent experiments.

To explore the molecular mechanisms of MeBavaC-mediated protection against cardiac hypertrophy, a model of cardiomyocyte hypertrophy was first established by exposing H9C2 cells to sodium succinate (1 mM) for 12, 24 and 48 h, respectively. TRITC-phalloidin staining revealed a time-dependent increase in cardiomyocyte size in the group that underwent sodium succinate treatment compared with the nontreatment group. In addition, sodium succinate treatment increased the relative cell cross-sectional area from 4,601±124 μm^2 at 0 h to 6,049±120 μm^2 at 48 h (n=3, counting 50 cells, Fig. 2A and B). Stimulation with sodium succinate for 6 h also promoted a nearly three-fold increase in cardiomyopathy-associated α-actinin mRNA expression without altering GATA4 expression (n=3, Fig. 2C and D). In addition, H9c2 cardiomyocytes were treated with sodium succinate for 60 min and immunofluorescence staining indicated a significant greater two-fold increase in NFATc4 content related to its nuclear translocation (n=3; counting 50 cells; Fig. 3A). However, treatment with the NFAT inhibitor VIVIT (2 μM) or the calcineurin inhibitor cyclosporine A (CsA, 5 nM) for 30 min prior to sodium succinate significantly blocked the nuclear translocation of NFATc4 induced by sodium succinate (n=3; counting 50 cells; Fig 3B), indicating that succinate activates the calcineurin-NFATc4 pathway in cardiomyocytes. Additionally, the induction of cardiomyocyte hypertrophy for 48 h by sodium succinate was blocked by VIVIT or CsA, with the relative cell cross-sectional area decreasing from 6,211±122 μm^2 in the succinate-stimulated model group to 4,529±90 μm^2 in the VIVIT-treated group or to 5,064±605 μm^2 in the CsA-treated group (n=3; counting 50 cells; Fig. 3B). The results demonstrated that succinate induced cardiomyocyte hypertrophy and activated NFATc4 nuclear translocation.

4'-O-methylbavachalcone prevents succinate-induced cardiomyocyte hypertrophy via NFATc4 signaling. To determine whether MeBavaC prevent cardiomyocyte hypertrophy, the present study investigated the effect of MeBavaC on succinate-induced cardiomyocyte hypertrophy. H9c2 cardiomyocytes were pretreated with MeBavaC at the concentrations of 1.25, 2.5 and 5 μM for 30 min. MeBavaC was found to inhibit NFATc4 nuclear translocation in a concentration-dependent manner. This inhibition was induced by sodium succinate for 60 min. NFATc4 nuclear translocation nearly returned to the prestimulation levels after 5 μM MeBavaC treatment (n=3; counting 50 cells; Fig. 4A). The inhibitory effect of MeBavaC on cardiomyocyte hypertrophy was determined by TRITC-phalloidin staining. Pretreatment with MeBavaC for 30 min effectively prevented cardiomyocyte hypertrophy induced by sodium succinate for 48 h, with an inhibition of

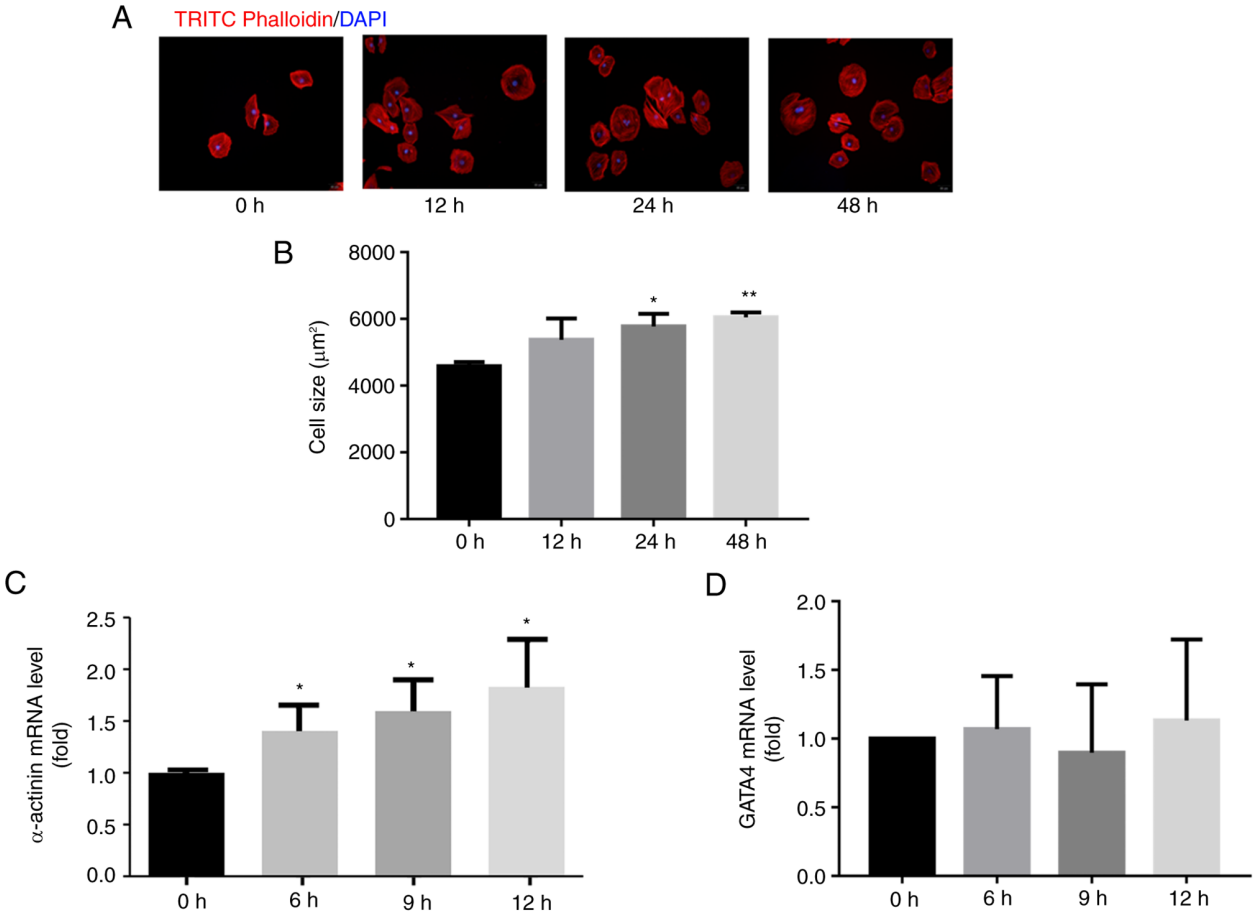

Figure 2. Succinate induced cardiomyocyte hypertrophy. (A and B) Time-dependent succinate-stimulated hypertrophy of H9c2 cells determined by TRITC-phalloidin staining (n=3 each, counting 50 cells). Magnification, x200. (C and D) Succinate stimulated mRNA expression of α-actinin and GATA4 measured using real-time quantitative PCR (n=3 each). Comparisons between groups were analyzed using Dunnett's multiple comparison test after one-way ANOVA. Data are expressed as mean ± standard deviation. *P<0.05 and **P<0.01 vs. 0 h group. TRITC, tetramethylrhodamine.

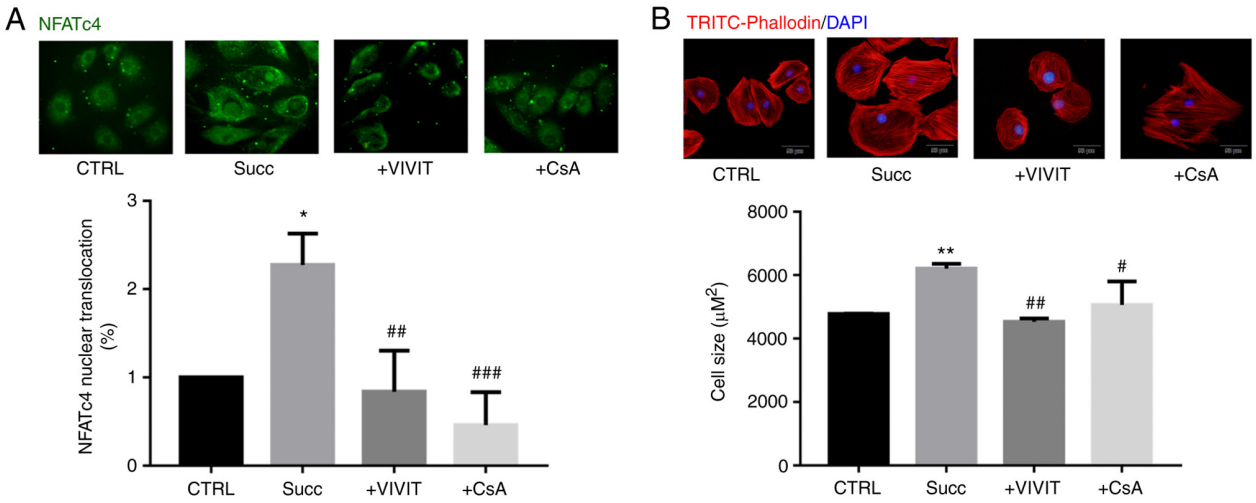

Figure 3. Succinate stimulated nuclear translocation of NFATc4 and its association with cardiomyocyte hypertrophy. (A) Immunofluorescence microscopy image of succinate-stimulated nuclear translocation of NFATc4 labeled with Alexa Fluor 488 (n=3 each; counting 50 cells). Magnification, x400. (B) Inhibitory effect of VIVIT and CsA on succinate-induced hypertrophy of H9c2 cardiomyocytes (n=3, counting 50 cells). Magnification, x200. Comparisons between groups were analyzed using Dunnett's multiple comparison test following one-way ANOVA. Data are expressed as mean ± standard deviation. *P<0.05 and **P<0.01 vs. control group; $^{\#}$P<0.05, $^{\#\#}$P<0.01 and $^{\#\#\#}$P<0.001 vs. succinate-stimulated group. NFATc, nuclear factor activated T cell.

up to 20% compared with the model group (n=3; counting 50 cells; Fig. 4B). RT-qPCR revealed that MeBavaC restored the gene expression of α-actinin induced by sodium succinate for 6 h, which is a hypertrophic marker (n=3; Fig. 4C).

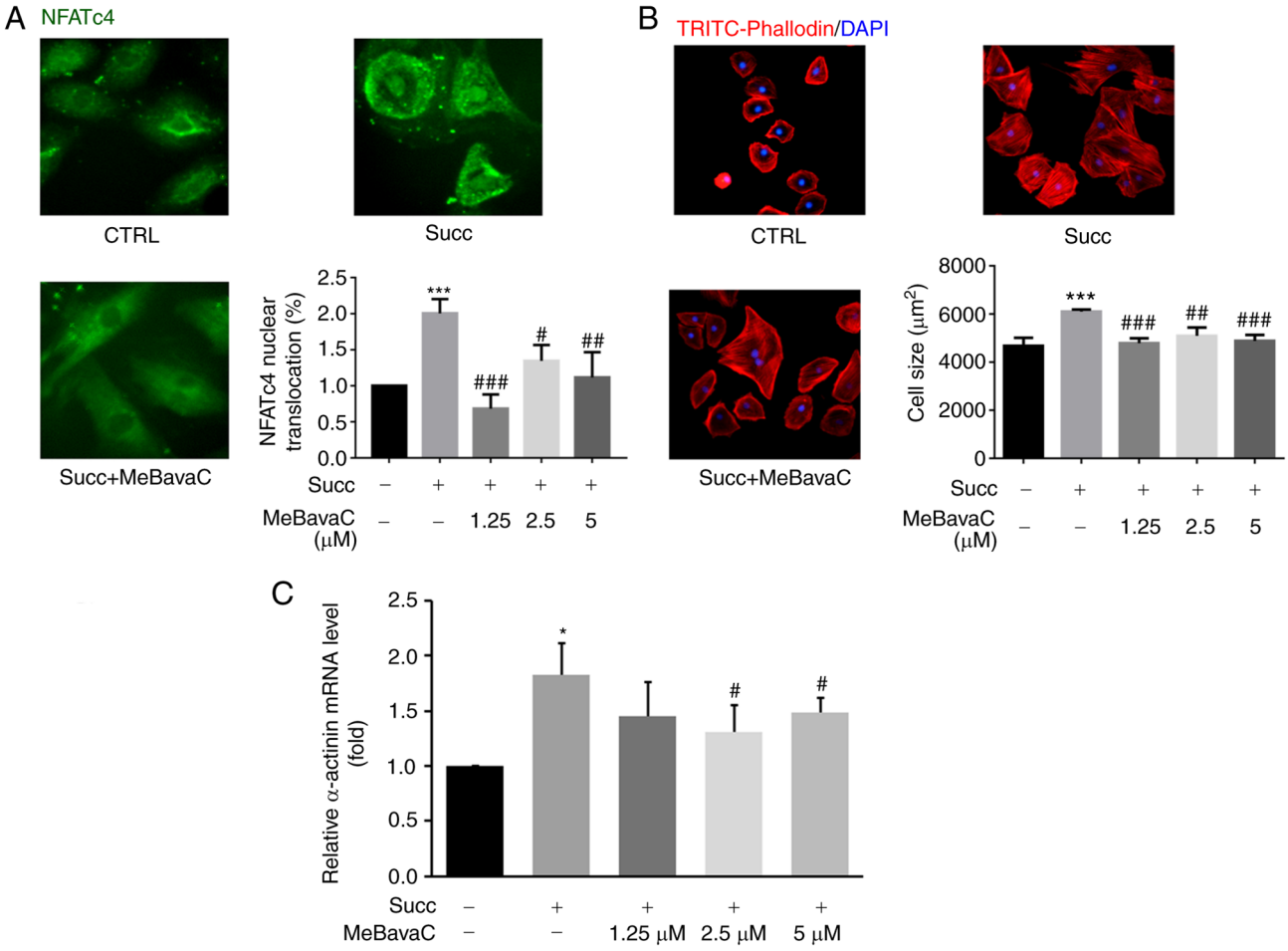

Figure 4. Inhibitory effect of MeBavaC on succinate-stimulated nuclear translocation of NFATc4 and cardiomyocyte hypertrophy. Effect of MeBavaC on (A) nuclear translocation of NFATc4 (magnification, x400) and (B) cell size (magnification, x200) imaged through immunofluorescence microscopy of succinate-induced hypertrophy of H9c2 cardiomyocytes (n=3; counting 50 cells). (C) Effect of MeBavaC on succinate-stimulated α-actinin mRNA expression in succinate-stimulated H9c2 cardiomyocytes (n=3). Comparisons between groups were analyzed using Dunnett's multiple comparison test following one-way ANOVA. Data are expressed as mean ± standard deviation. *P<0.05, and ***P<0.001 vs. control group; $^{\#}$P<0.05, $^{\#\#}$P<0.01 and $^{\#\#\#}$P<0.001 vs. succinate-stimulated group. MeBavaC, 4'-O-methylbavachalcone; TRITC, tetramethylrhodamine.

Role of MAPK on 4'-O-methylbavachalcone in improving cardiomyocyte hypertrophy. The phosphorylation activities of ERK1/2 and JNK kinases, two essential members of MAPK signaling, were activated by sodium succinate for 15 min as detected using western blotting, but not by p38 kinase (n=3; Fig. 5A-C). Pretreatment with MeBavaC for 30 min significantly inhibited ERK1/2 and JNK phosphorylation with a maximum inhibition of ~15 and 40%, respectively (n=3; Fig. 5A-C). However, sodium succinate-induced cardiomyocyte hypertrophy was blocked by 30 min of pretreatment of the ERK1/2 pathway inhibitor PD98059 (20 μM), but not the JNK pathway inhibitor SP600125 (20 μM), as indicated by a decreased cardiomyocytes size (~30%; n=3; counting 50 cells; Fig. 5D and E). These results indicated that ERK1/2 signaling partly serves a role in mediating succinate-induced cardiomyocyte hypertrophy.

Molecular docking analysis of 4'-O-methylbavachalcone and the SUCNR1 receptor. To elucidate the binding mechanism of MeBavaC on SUCNR1 in detail, a docking simulation analysis was performed. As presented in Fig. 6A, MeBavaC and succinate bound SUCNR1 at extremely close position. Binding to both the Cys168 and Val169 groups of the SUCNR1 receptor, succinate was bound via hydrogen bonds, whereas MeBavaC was bound via the alkyl and Pi-alkyl groups (Fig. 6B and C). Markedly, MeBavaC was predicted to be more compatible with the orthosteric site of SUCNR1 than was succinate, with the two having a docking score of -8.1 and -4.7 kcal/mol, respectively. The carbonyl of succinate is integrally docked to a pseudooxyanion whole (Fig. 6C and D), which is generally a proteinaceous substruction preferring multiform oxygen atoms and consists of Tyr26, Tyr29 and Arg276. Nevertheless, MeBavaC formed stable Pi-cation with Lys18 as well as Pi-Alkyl with Leu75. Taken together, these results indicate that MeBavaC inhibited SUCNR1 activity.

Discussion

Succinate is an intermediate product of mitochondrial metabolism and mitochondrial damage results in succinate leakage. A number of cardiovascular events, such as myocardial infarction, atrial fibrillation and heart failure, promote succinate leakage from cardiomyocytes (20,37-39). Succinate is the only metabolite whose levels are significantly

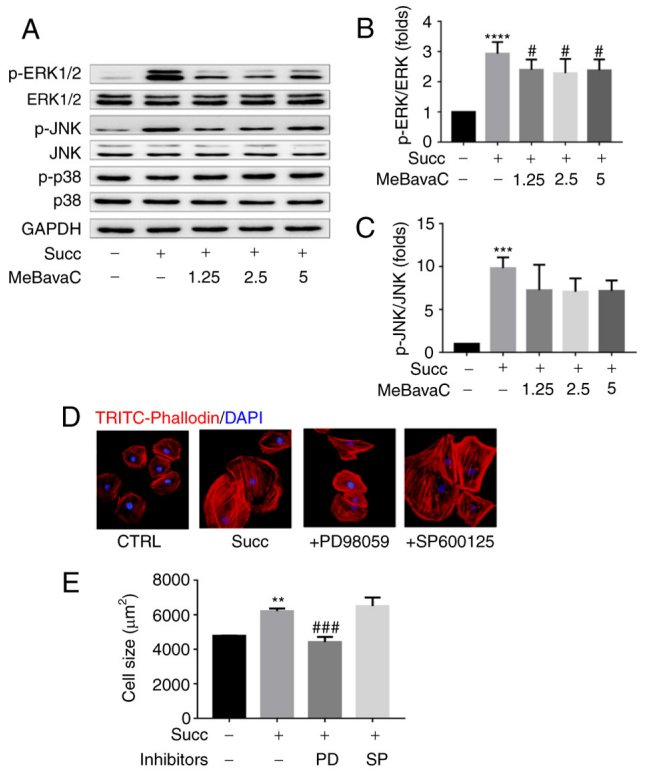

Figure 5. Effect of MeBavaC on succinate-stimulated MAPK activity and association with cardiomyocyte hypertrophy. (A, B and C) Effects of MeBavaC on succinate-stimulated MAPK phosphorylation levels (n=3). (D and E) Effects of ERK1/2 and JNK pathways inhibitors (PD98059 and SP600125) on succinate-induced hypertrophy of H9c2 cardiomyocytes (n=3; counting 50 cells). Magnification, x200. Comparisons between groups were completed using Dunnett's multiple comparison test after one-way ANOVA. Data are analyzed as mean ± standard deviation. **P<0.01, ***P<0.001 and ****P<0.0001 vs. control group; $^{\#}$P<0.05 and $^{\#\#\#}$P< 0.001 vs. the succinate-stimulated group. MeBavaC: 4'-O-methylbavachalcone; p-, phosphorylated; TRITC, tetramethylrhodamine.

increased in the coronary sinus compared with in the venous blood in patients with STEMI, suggesting that it is released in the heart. Succinate concentrations in arterial, coronary sinus and peripheral venous blood are higher in patients with STEMI than in patients without STEMI or with stable angina pectoris (20). The mean succinate concentration in the coronary sinus blood of patients with STEMI is reported to be 2.73 μM, which is ~ twice that of patients with angina pectoris and without STEMI (20). In addition, enhanced levels of succinate are closely associated with an increased risk of atrial fibrillation due to the extreme quartiles of TAC metabolites in patients with atrial fibrillation (37). Elevated myocardial energy expenditure has been associated with reduced left ventricular ejection fraction and an independent predictor of cardiovascular mortality. In patients with heart failure, serum succinate concentrations also significantly increased with increasing myocardial energy expenditure elevation (38). Succinate accumulates during ischemia and two-thirds of ischemic succinate accumulation is extracellular (40). In addition, succinate produced by gut microbiota is also directly related to the development of cardiovascular disease (41,42). Compared with healthy animals, the blood succinate concentration of spontaneously hypertensive rats, ob/ob mice, fa/fa rats and db/db mice was significantly increased. Therefore, ultra-high succinate concentrations in the blood may be involved in the occurrence of numerous cardiovascular events. In the present study, 1 mM of sodium succinate incubated with H9C2 cardiomyocytes for 48 h promoted cardiomyocyte hypertrophy and increased the expression of cardiomyopathy-associated gene α-actinin (Fig. 2), which is partly consistent with the finding of Aguiar *et al* (24). Their findings indicate that intravenous injection of 0.066 mg/kg of sodium succinate salt into 8-week-old Wistar rats with cardiac ischemia once daily for 5 days can lead to cardiac hypertrophy. They further stimulated cardiomyocytes from neonatal (3-5 days old) Wistar rats with 1 mM of sodium succinate, which triggered hypertrophy of cardiac cardiomyocytes by activating the SUCNR1 receptor and through phosphorylation of ERK1/2 and expression of CaMKIIδ (24). *In vivo* experiments in rats have also indicated that succinate enhanced pressure overload-induced right ventricular hypertrophy. Yang *et al* (43) selected three succinate concentrations of 30, 50 and 100 mg/kg/day in the pre-experiment. As rats given a dose of 100 mg/kg/day succumbed before the end of the experiment, 50 mg/kg/day was chosen as the follow-up experimental dose. Stimulation with 50 mg/kg/day succinate resulted in right ventricular hypertrophy in rats and enhanced ANP gene expression and Akt signaling (43). High sodium succinate concentrations (1 mM) also promote platelet aggregation and cross-cellular biosynthesis of leukotriene C_4 by activating SUCNR1 (36).

Succinate is primarily sensed by the G-protein-coupled receptor SUCNR1, which serves a role in extracellular metabolic stress signaling. SUCNR1 is widely expressed in various tissues, including the kidney, liver, heart and retinal, resulting in a wide range of physiological and pathological effects. The increase in blood succinate concentration in hypertension, obesity and diabetes model animals is consistent with SUCNR1 activation (19). SUCNR1 serves specific proinflammatory and antiinflammation roles in macrophages. When SUCNR1-expressing macrophages are activated by inflammatory signals, the accumulated succinate is released into the extracellular milieu. SUCNR1 activation binding to autocrine or paracrine succinate can perpetuate inflammation by enhancing IL-1β production in macrophages (44). Several cardiac hypertrophy-related signals, including phosphorylation of ERK1/2, expression of CaMKIIδ and translocation of histone deacetylase 5 into cytoplasm, are triggered by SUCNR1 activation and serve critical roles in the hypertrophic remodeling of the myocardium (24), indicating that cardiac hypertrophy is induced in a SUCNR1-dependent manner. SUCNR1 stimulation activates Gαi and initiates Gαq activity (45,46), which is required to trigger intracellular Ca^{2+} flux. SUCNR1 requires PLCβ activation to increase intracellular Ca^{2+} through an inositol phosphate-dependent mechanism (47). The canonical Gi-Gβγ-$Ca2^{+}$ signaling also requires the participation of the Gαq subunit in living cells (48). Ca^{2+} flux is the upstream signal of the CaMKIIδ and calcineurin-NFAT pathways and abnormal Ca^{2+} flux is one of the molecular bases of cardiac hypertrophy (12,49,50). The results of the present study also revealed that succinate treatment promoted cardiomyocyte size enlargement and increased α-actinin expression (Figs. 2 and 4). The gene α-actinin is associated with dilated cardiomyopathy, impaired ventricular diastolic function and cardiac hypertrophy (51,52) and

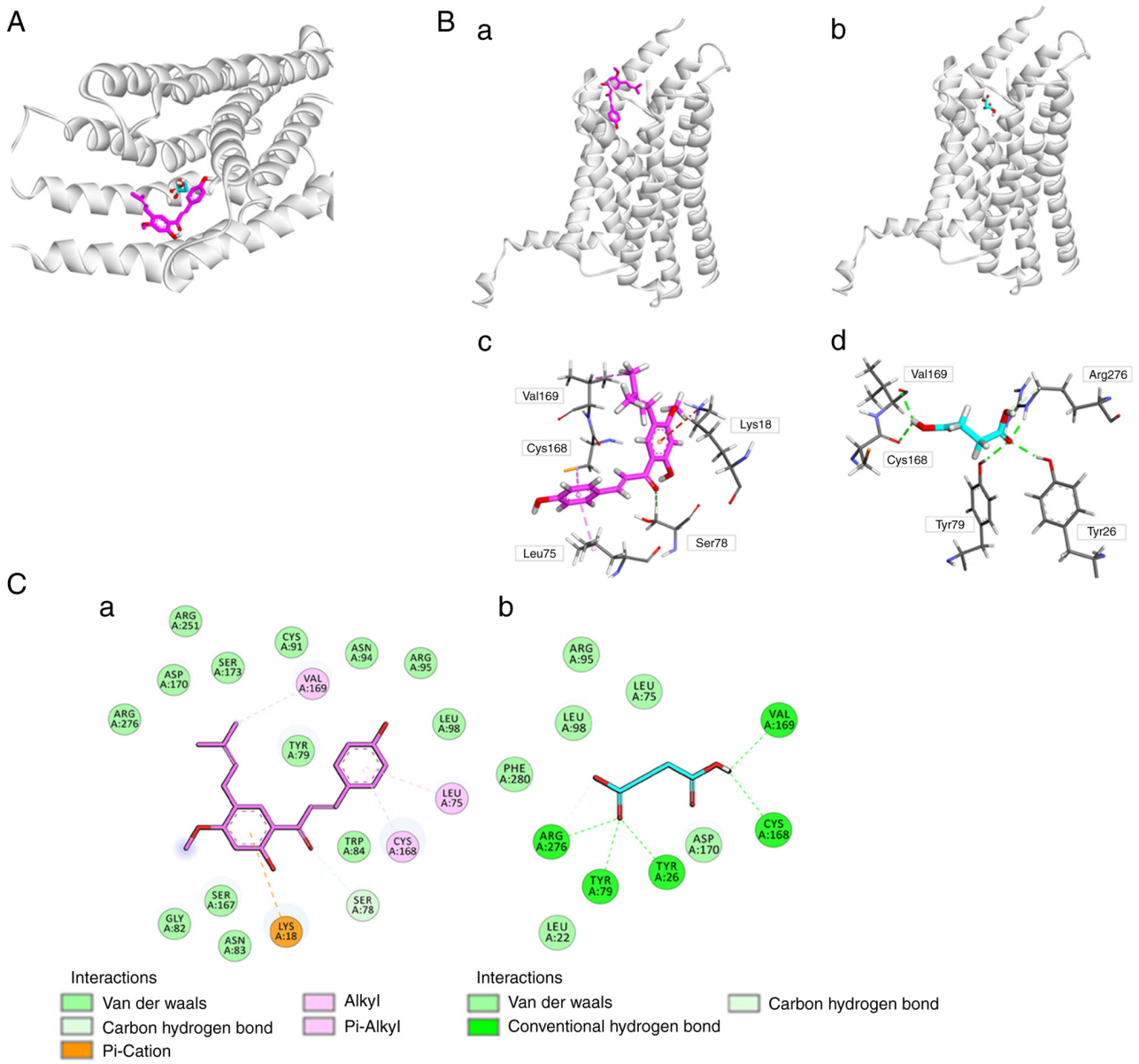

D

Feature key	Position(s)	Description	Succinate	MeBavaC
Topological domain	5 – 31	Extracellular	Tyr26	Lys18
Transmembrane	60 – 80	Helical; Name=2	Tyr79	Leu75, Ser78
Topological domain	81 – 103	Extracellular	Arg95	
Topological domain	159 – 185	Extracellular	Cys168 Val169	Cys168 Val169
Topological domain	252 – 281	Extracellular	Arg276	

Figure 6. Molecular docking analysis of SUCNR1 with MeBavaC and succinate. (A) The orthosteric site of SUCNR1 (white) binding MeBavaC (magenta) and succinate (cyan). The docking modes were predicted by AutoDock Vina. (Ba and Bb) Overall stereoscopic docking modes of MeBavaC (magenta) and succinate (cyan) upon SUCNR1 (white); (Bc and Bd) Receptor-ligand interaction features of MeBavaC and succinate on the orthosteric site of SUCNR1; (Ca and Cb) 2D receptor-ligand interaction analysis of MeBavaC (magenta) or succinate (cyan) on the orthosteric site of SUCNR1; (D) Functional bond site for UCNR1 binding to MeBavaC or succinate. SUCNR1, succinate receptor 1; MeBavaC, 4'-O-methylbavachalcone.

α-actinin-1 promotes the activity of the L-type Ca^{2+} channel Cav 1.2 (53,54), which regulates cardiac hypertrophy (55,56). Together, these findings indicate the presence of at least two pathways by which stimulation of SUCNR1 increase intracellular Ca^{2+} flux to contribute to cardiac hypertrophy; by triggering Gαq activity and PLCβ and activating the L-type Ca^{2+} channel Cav 1.2 opening.

Calcineurin-NFAT signaling is an important regulatory pathway of cardiac hypertrophy. However, whether succinate can activate calcineurin-NFAT signaling has not been

determined. To this end, the nuclear translocation of NFATc4 was observed in cardiomyocytes after they were treated with succinate. The results suggested that succinate-induced cardiomyocyte hypertrophy is mediated by the calcineurin-NFATc4 signaling (Fig. 3). Indeed, four NFAT members (NFATc1-c4) are expressed in cardiomyocytes; they trigger nuclear translocation upon calcineurin activation and yet promote cardiomyocyte hypertrophy (14,57). The data from the present study also indicated that succinate activated ERK1/2 and JNK signaling and that inhibition of ERK1/2 signaling, but not of JNK signaling, attenuated cardiomyocyte hypertrophy (Fig. 5). ERK1/2 stimulation induces cardiac hypertrophy, whereas JNK activation in cardiomyocytes directly antagonizes activated NFAT signaling (15,58). In cultured cardiomyocytes, ERK1/2 signaling inhibition attenuates hypertrophy induced by activated calcineurin. Nevertheless, the targeted inhibition of ERK1/2 signaling does not directly affect calcineurin-NFAT activation (58).

Fructus Psoraleae mainly contains coumarins, terpene phenols and prenylflavonoids, which are the material basis of drug therapy. MeBavaC is an active component of prenylflavonoids. The authors previously reviewed the mechanisms of five major psoralea prenylflavonoids and their multiple effects including anti-inflammation, cardiovascular protection, neuroprotection, osteoporosis improvement and intervention on diabetes and obesity (26). No cardiovascular pharmacological study of MeBavaC has been conducted and the present study revealed its mechanism in preventing cardiac hypertrophy. The results demonstrated that MeBavaC blocks both calcineurin-NFAT and ERK1/2 signaling and inhibits succinate-induced cardiomyocyte hypertrophy (Figs. 4 and 5). A number of prenylflavonoids, such as xanthohumol and icariin, have multiple cardiovascular protection functions. Xanthohumol inhibits abnormal ryanodine receptor Ca^{2+} release, possesses antiarrhythmic properties, attenuates isoproterenol-induced cardiac hypertrophy and fibrosis and protects rat myocardia from ischemia/reperfusion injury-induced ferroptosis (59-61). Icariin inhibits isoproterenol-induced cardiomyocyte hypertrophic injury and severe heart failure, protects cardiomyocytes from ischemia/reperfusion injury and attenuates Ang II-induced H9c2 cardiomyocyte hypertrophy and apoptosis (62-65). In Fructus Psoraleae, only bakuchiol, a terpene phenol, was reported to block aortic banding-induced cardiac hypertrophy by blocking the NF-κB signaling pathway and to attenuate pressure overload-induced fibrosis and inflammation (66).

In 2011 year, compounds numbered 2C, 4C and 5G were identified as potent and selective antagonists for human SUCNR1 (67). Another group recently discovered an optimized SUCNR1 antagonist scaffold to improve oral exposure by designing Zwitterionic Derivatives with salt bridges (68). Using a humanized rat construct, the X-ray structure of optimized compound 20 binding to SUCNR1 was determined (67). On this published humanized rat SUCNR1 construct, the team also confirmed the structure of another antagonist, NF-56-EJ40, in complex with its receptor, SUCNR1 (34). In the present study, molecular docking analysis indicated that MeBavaC binds to the orthosteric site of succinate receptor SUCNR1 through alkyl and Pi-alkyl, which are more compatible than succinate with a higher docking score (Fig. 6). When binding to the pseudo-oxyanionic protein subunit group of SUCNR1, MeBavaC formed stable Pi-cation complexes with Lys18, as well as Pi-alkyl bonds with Leu75 (Fig. 6). The results indicated that MeBavaC inhibited SUCNR1 activity.

The results of the present study revealed that succinate stimulated cardiomyocyte hypertrophy through the calcineurin-NFATc4 and ERK1/2 pathways. MeBavaC ameliorated succinate-induced cardiomyocyte hypertrophy mediated by calcineurin-NFATc4 and ERK1/2 pathways. Molecular docking analysis indicated that MeBavaC had a certain affinity for the succinate receptor SUCNR1 and the ability to inhibit SUCNR1 binding with succinate. Therefore, MeBavaC has fully demonstrated the potential ability to improve myocardial hypertrophy and heart failure, associated with elevated myocardial energy expenditure and an increased extra serum succinate concentration.

Acknowledgements

Not applicable.

Funding

The present study was supported by grants from the Specialized Research Fund for the National Natural Science Foundation of China (grant no. 81973511).

Availability of data and materials

The datasets used and/or analyzed during the current study are available from the corresponding author on reasonable request.

Authors' contributions

HS implemented most of the experiments, data collation and statistics and wrote the first draft of the manuscript. GZ implemented the molecular docking research, data collation and statistical analyses and wrote the first draft of the molecular docking section of the manuscript. SL participated in part of the experimental design, gave technical guidance on cardiomyocyte culture, conducted financial management and assisted in the revision of the manuscript. JL provided experimental design for the Western blot, validated some of the real-time PCR experiments, provided technical guidance on microscopy and monitored the progress of the experiments, and assisted in the revision of the manuscript. JWX proposed the research idea, obtained financial support and revised and finalized the manuscript. HS, GZ and JL confirm the authenticity of all the raw data. All authors read and approved the final manuscript.

Ethics approval and consent to participate

Not applicable.

Patient consent for publication

Not applicable.

Competing interests

The authors declare that they have no competing interests

References

1. Gould KL, Lipscomb K, Hamilton GW and Kennedy JW: Left ventricular hypertrophy in coronary artery disease. A cardiomyopathy syndrome following myocardial infarction. Am J Med 55: 595-601, 1973.
2. Momiyama Y, Suzuki Y, Ohsuzu F, Atsumi Y, Matsuoka K and Kimura M: Left ventricular hypertrophy and diastolic dysfunction in mitochondrial diabetes. Diabetes Care 24: 604-605, 2001.
3. De Simone G, Devereux RB, Roman MJ, Alderman MH and Laragh JH: Relation of obesity and gender to left ventricular hypertrophy in normotensive and hypertensive adults. Hypertension 23: 600-606, 1994.
4. Li H, He C, Feng J, Zhang Y, Tang Q, Bian Z, Bai X, Zhou H, Jiang H, Heximer SP, *et al*: Regulator of G protein signaling 5 protects against cardiac hypertrophy and fibrosis during biomechanical stress of pressure overload. Proc Natl Acad Sci USA 107: 13818-13823, 1994.
5. Cibi DM, Bi-Lin KW, Shekeran SG, Sandireddy R, Tee N, Singh A, Wu Y, Srinivasan DK, Kovalik JP, Ghosh S, *et al*: Prdm16 deficiency leads to age-dependent cardiac hypertrophy, adverse remodeling, mitochondrial dysfunction, and heart failure. Cell Rep 33: 108288, 2020.
6. Ritterhoff J, Young S, Villet O, Shao D, Neto FC, Bettcher LF, Hsu YA, Kolwicz SC Jr, Raftery D and Tian R: Metabolic remodeling promotes cardiac hypertrophy by directing glucose to aspartate biosynthesis. Circ Res 126: 182-196, 2020.
7. Zhang T and Brown JH: Role of Ca^{2+}/calmodulin-dependent protein kinase II in cardiac hypertrophy and heart failure. Cardiovasc Res 63: 476-486, 2004.
8. Yang L, Cao J, Ma J, Li M and Mu Y: Differences in the microcirculation disturbance in the right and left ventricles of neonatal rats with hypoxic pulmonary hypertension. Microvasc Res 135: 104129, 2021.
9. Liu HB, Yang BF and Dong DL: Calcineurin and electrical remodeling in pathologic cardiac hypertrophy. Trends Cardiovasc Med 20: 148-153, 2010.
10. Molkentin JD: Calcineurin and beyond: Cardiac hypertrophic signaling. Circ Res 87: 731-738, 2000.
11. Crabtree GR: Generic signals and specific outcomes: Signaling through Ca^{2+}, calcineurin, and NF-AT. Cell 96: 611-614, 1999.
12. Wilkins BJ, Dai YS, Bueno OF, Parsons SA, Xu J, Plank DM, Jones F, Kimball TR and Molkentin JD: Calcineurin/NFAT coupling participates in pathological, but not physiological, cardiac hypertrophy. Circ Res 94: 110-118, 2004.
13. Mathew S, Mascareno E and Siddiqui MA: A ternary complex of transcription factors, Nished and NFATc4, and co-activator p300 bound to an intronic sequence, intronic regulatory element, is pivotal for the up-regulation of myosin light chain-2v gene in cardiac hypertrophy. J Biol Chem 279: 41018-41027, 2004.
14. Van Rooij E, Doevendans PA, de Theije CC, Babiker FA, Molkentin JD and de Windt LJ: Requirement of nuclear factor of activated T-cells in calcineurin-mediated cardiomyocyte hypertrophy. J Biol Chem 277: 48617-48626, 2002.
15. Molkentin JD: Calcineurin-NFAT signaling regulates the cardiac hypertrophic response in coordination with the MAPKs. Cardiovasc Res 63: 467-475, 2004.
16. Pin F, Barreto R, Couch ME, Bonetto A and O'Connell TM: Cachexia induced by cancer and chemotherapy yield distinct perturbations to energy metabolism. J Cachexia Sarcopenia Muscle 10: 140-154, 2019.
17. Lehwald N, Tao GZ, Jang KY, Papandreou I, Liu B, Liu B, Pysz MA, Willmann JK, Knoefel WT, Denko NC and Sylvester KG: β-Catenin regulates hepatic mitochondrial function and energy balance in mice. Gastroenterology 143: 754-764, 2012.
18. Björntorp P: The oxidation of fatty acids combined with albumin by isolated rat liver mitochondria. J Biol Chem 241: 1537-1543, 1966.
19. Sadagopan N, Li W, Roberds SL, Major T, Preston GM, Yu Y and Tones MA: Circulating succinate is elevated in rodent models of hypertension and metabolic disease. Am J Hypertens 20: 209-1215, 2007.
20. Kohlhauer M, Dawkins S, Costa ASH, Lee R, Young T, Pell VR, Choudhury RP, Banning AP, Kharbanda RK; Oxford Acute Myocardial Infarction (OxAMI) Study, *et al*: Metabolomic profiling in acute ST-segment-elevation myocardial infarction identifies succinate as an early marker of human ischemia-reperfusion injury. J Am Heart Assoc 7: e007546, 2018.
21. de Castro Fonseca M, Aguiar CJ, da Rocha Franco JA, Gingold RN and Leite MF: GPR91: Expanding the frontiers of Krebs cycle intermediates. Cell Commun Signal 14: 3, 2016.
22. Li X, Xie L, Qu X, Zhao B, Fu W, Wu B and Wu J: GPR91, a critical signaling mechanism in modulating pathophysiologic processes in chronic illnesses. FASEB J 34: 13091-13105, 2020.
23. Yang L, Yu D, Mo R, Zhang J, Hua H, Hu L, Feng Y, Wang S, Zhang WY, Yin N and Mo XM: The succinate receptor GPR91 is involved in pressure overload-induced ventricular hypertrophy. PLoS One 11: e0147597, 2016.
24. Aguiar CJ, Rocha-Franco JA, Sousa PA, Santos AK, Ladeira M, Rocha-Resende C, Ladeira LO, Resende RR, Botoni FA, Melo MB, *et al*: Succinate causes pathological cardiomyocyte hypertrophy through GPR91 activation. Cell Commun Signal 12: 78, 2014.
25. Chinese Pharmacopoeia Commission, 2020. Psoraleae Fructus. In: Pharmacopoeia of the People's Republic of China. China Medical Science Press, Beijing. pp 195.
26. Zhou YT, Zhu L, Yuan Y, Ling S and Xu JW: Effects and mechanisms of five psoralea prenylflavonoids on aging-related diseases. Oxid Med Cell Longev 2020: 2128513, 2020.
27. Yan C, Wu Y, Weng Z, Gao Q, Yang G, Chen Z, Cai B and Li W: Development of an HPLC method for absolute quantification and QAMS of flavonoids components in Psoralea corylifolia L. J Anal Methods Chem 2015: 792637, 2015.
28. Kim DW, Seo KH, Curtis-Long MJ, Oh KY, Oh JW, Cho JK, Lee KH and Park KH: Phenolic phytochemical displaying SARS-CoV papain-like protease inhibition from the seeds of Psoralea corylifolia. J Enzyme Inhib Med Chem 29: 59-63, 2014.
29. Cooper JA: Effects of cytochalasin and phalloidin on actin. J Cell Biol 105: 1473-1478, 1987.
30. Jia G, Liang C, Li W and Dai H: MiR-410-3p facilitates angiotensin II-induced cardiac hypertrophy by targeting Smad7. Bioengineered 13: 119-127, 2022.
31. Sugawara Y, Kamioka H, Honjo T, Tezuka K and Takano-Yamamoto T: Three-dimensional reconstruction of chick calvarial osteocytes and their cell processes using confocal microscopy. Bone 36: 877-883, 2005.
32. Livak KJ and Schmittgen TD: Analysis of relative gene expression data using real-time quantitative PCR and the 2(Delta Delta C(T)) method. Methods 25: 402-408, 2001.
33. Burley SK, Berman HM, Kleywegt GJ, Markley JL, Nakamura H and Velankar S: Protein data bank (PDB): The single global macromolecular structure archive. Methods Mol Biol 1607: 627-641, 2017.
34. Haffke M, Fehlmann D, Rummel G, Boivineau J, Duckely M, Gommermann N, Cotesta S, Sirockin F, Freuler F, Littlewood-Evans A, *et al*: Structural basis of species-selective antagonist binding to the succinate receptor. Nature 574: 581-585, 2019.
35. Trauelsen M, Ulven ER, Hjorth SA, Brvar M, Monaco C, Frimurer TM and Schwartz TW: Receptor structure-based discovery of non-metabolite agonists for the succinate receptor GPR91. Mol Metab 6: 1585-1596, 2017.
36. Tang X, Fuchs D, Tan S, Trauelsen M, Schwartz TW, Wheelock CE, Li N and Haeggström JZ: Activation of metabolite receptor GPR91 promotes platelet aggregation and transcellular biosynthesis of leukotriene C4. J Thromb Haemost 18: 976-984, 2020.
37. Bulló M, Papandreou C, García-Gavilán J, Ruiz-Canela M, Li J, Guasch-Ferré M, Toledo E, Clish C, Corella D, Estruch R, *et al*: Tricarboxylic acid cycle related-metabolites and risk of atrial fibrillation and heart failure. Metabolism 125: 154915, 2021.
38. Du Z, Shen A, Huang Y, Su L, Lai W, Wang P, Xie Z, Xie Z, Zeng Q, Ren H and Xu D: 1H-NMR-based metabolic analysis of human serum reveals novel markers of myocardial energy expenditure in heart failure patients. PLoS One 9: e88102, 2014.
39. Yao H, Shi P, Zhang L, Fan X, Shao Q and Cheng Y: Untargeted metabolic profiling reveals potential biomarkers in myocardial infarction and its application. Mol Biosyst 6: 1061-1070, 2010.
40. Zhang J, Wang YT, Miller JH, Day MM, Munger JC and Brookes PS: Accumulation of succinate in cardiac ischemia primarily occurs via canonical Krebs cycle activity. Cell Rep 23: 2617-2628, 2018.
41. Galla S, Chakraborty S, Cheng X, Yeo JY, Mell B, Chiu N, Wenceslau CF, Vijay-Kumar M and Joe B: Exposure to amoxicillin in early life is associated with changes in gut microbiota and reduction in blood pressure: Findings from a study on rat dams and offspring. J Am Heart Assoc 9: e014373, 2020.

42. Serena C, Ceperuelo-Mallafré V, Keiran N, Queipo-Ortuño MI, Bernal R, Gomez-Huelgas R, Urpi-Sarda M, Sabater M, Pérez-Brocal V, Andrés-Lacueva C, *et al*: Elevated circulating levels of succinate in human obesity are linked to specific gut microbiota. ISME J 12: 1642-1657, 2018.
43. Yang L, Yu D, Fan HH, Feng Y, Hu L, Zhang WY, Zhou K and Mo XM: Triggering the succinate receptor GPR91 enhances pressure overload-induced right ventricular hypertrophy. Int J Clin Exp Pathol 7: 5415-5428, 2014.
44. Littlewood-Evans A, Sarret S, Apfel V, Loesle P, Dawson J, Zhang J, Muller A, Tigani B, Kneuer R, Patel S, *et al*: GPR91 senses extracellular succinate released from inflammatory macrophages and exacerbates rheumatoid arthritis. J Exp Med 213: 1655-1662, 2016.
45. Ko SH, Choi GE, Oh JY, Lee HJ, Kim JS, Chae CW, Choi D and Han HJ: Succinate promotes stem cell migration through the GPR91-dependent regulation of DRP1-mediated mitochondrial fission. Sci Rep 7: 12582, 2017.
46. Trauelsen M, Hiron TK, Lin D, Petersen JE, Breton B, Husted AS, Hjorth SA, Inoue A, Frimurer TM, Bouvier M, *et al*: Extracellular succinate hyperpolarizes M2 macrophages through SUCNR1/GPR91-mediated Gq signaling. Cell Rep 35: 109246, 2021.
47. Sundström L, Greasley PJ, Engberg S, Wallander M and Ryberg E: Succinate receptor GPR91, a Gα(i) coupled receptor that increases intracellular calcium concentrations through PLCβ. FEBS Lett 587: 2399-2404, 2013.
48. Pfeil EM, Brands J, Merten N, Vögtle T, Vescovo M, Rick U, Albrecht IM, Heycke N, Kawakami K, Ono Y, *et al*: Heterotrimeric G protein subunit Gαq is a master switch for Gβγ-mediated calcium mobilization by Gi-coupled GPCRs. Mol Cell 80: 940-954.e6, 2020.
49. Backs J, Backs T, Neef S, Kreusser MM, Lehmann LH, Patrick DM, Grueter CE, Qi X, Richardson JA, Hill JA, *et al*: The delta isoform of CaM kinase II is required for pathological cardiac hypertrophy and remodeling after pressure overload. Proc Natl Acad Sci USA 106: 2342-2347, 2009.
50. Pieske B, Kretschmann B, Meyer M, Holubarsch C, Weirich J, Posival H, Minami K, Just H and Hasenfuss G: Alterations in intracellular calcium handling associated with the inverse force-frequency relation in human dilated cardiomyopathy. Circulation 92: 1169-1178, 1995.
51. Prondzynski M, Lemoine MD, Zech AT, Horváth A, Di Mauro V, Koivumäki JT, Kresin N, Busch J, Krause T, Krämer E, *et al*: Disease modeling of a mutation in α-actinin 2 guides clinical therapy in hypertrophic cardiomyopathy. EMBO Mol Med 11: e11115, 2019.
52. Sheng JJ, Feng HZ, Pinto JR, Wei H and Jin JP: Increases of desmin and α-actinin in mouse cardiac myofibrils as a response to diastolic dysfunction. J Mol Cell Cardiol 99: 218-229, 2016.
53. Hall DD, Dai S, Tseng PY, Malik Z, Nguyen M, Matt L, Schnizler K, Shephard A, Mohapatra DP, Tsuruta F, *et al*: Competition between α-actinin and Ca^{2+}-calmodulin controls surface retention of the L-type Ca^{2+} channel Ca(V)1.2. Neuron 78: 483-497, 2013.
54. Turner M, Anderson DE, Bartels P, Nieves-Cintron M, Coleman AM, Henderson PB, Man KNM, Tseng PY, Yarov-Yarovoy V, Bers DM, *et al*: α-Actinin-1 promotes activity of the L-type Ca2+ channel Cav 1.2. EMBO J 39: e102622, 2020.
55. Han JW, Kang C, Kim Y, Lee MG and Kim JY: Isoproterenol-induced hypertrophy of neonatal cardiac myocytes and H9c2 cell is dependent on TRPC3-regulated CaV1.2 expression. Cell Calcium 92: 102305, 2020.
56. Hu Z, Wang JW, Yu D, Soon JL, de Kleijn DP, Foo R, Liao P, Colecraft HM and Soong TW: Aberrant splicing promotes proteasomal degradation of L-type Cav1.2 calcium channels by competitive binding for Cavβ subunits in cardiac hypertrophy. Sci Rep 6: 35247, 2016.
57. Molkentin JD, Lu JR, Antos CL, Markham B, Richardson J, Robbins J, Grant SR and Olson EN: A calcineurin-dependent transcriptional pathway for cardiac hypertrophy. Cell 93: 215-228, 1998.
58. Sanna B, Bueno OF, Dai YS, Wilkins BJ and Molkentin JD: Direct and indirect interactions between calcineurin-NFAT and MEK1-extracellular signal-regulated kinase 1/2 signaling pathways regulate cardiac gene expression and cellular growth. Mol Cell Biol 25: 865-878, 2005.
59. Arnaiz-Cot JJ, Cleemann L and Morad M: Xanthohumol modulates calcium signaling in rat ventricular myocytes: Possible antiarrhythmic properties. J Pharmacol Exp Ther 360: 239-248, 2017.
60. Lin JH, Yang KT, Lee WS, Ting PC, Luo YP, Lin DJ, Wang YS and Chang JC: Xanthohumol protects the rat myocardium against ischemia/reperfusion injury-induced ferroptosis. Oxid Med Cell Longev 2022: 9523491, 2022.
61. Sun TL, Li WQ, Tong XL, Liu XY and Zhou WH: Xanthohumol attenuates isoprenaline-induced cardiac hypertrophy and fibrosis through regulating PTEN/AKT/mTOR pathway. Eur J Pharmacol 891: 173690, 2021.
62. Hu L, Wang Z, Li H, Wei J, Tang F, Wang Q, Wang J, Zhang X and Zhang Q: Icariin inhibits isoproterenol-induced cardiomyocyte hypertropic injury through activating autophagy via the AMPK/mTOR signaling pathway. Biochem Biophys Res Commun 593: 65-72, 2022.
63. Song YH, Cai H, Gu N, Qian CF, Cao SP and Zhao ZM: Icariin attenuates cardiac remodelling through down-regulating myocardial apoptosis and matrix metalloproteinase activity in rats with congestive heart failure. J Pharm Pharmacol 63: 541-549, 2011.
64. Wu B, Feng JY, Yu LM, Wang YC, Chen YQ, Wei Y, Han JS, Feng X, Zhang Y, Di SY, *et al*: Icariin protects cardiomyocytes against ischaemia/reperfusion injury by attenuating sirtuin 1-dependent mitochondrial oxidative damage. Br J Pharmacol 175: 4137-4153, 2018.
65. Zhou H, Yuan Y, Liu Y, Deng W, Zong J, Bian ZY, Dai J and Tang QZ: Icariin attenuates angiotensin II-induced hypertrophy and apoptosis in H9c2 cardiomyocytes by inhibiting reactive oxygen species-dependent JNK and p38 pathways. Exp Ther Med 7: 1116-1122, 2014.
66. Wang Z, Gao L, Xiao L, Kong L, Shi H, Tian X and Zhao L: Bakuchiol protects against pathological cardiac hypertrophy by blocking NF-κB signaling pathway. Biosci Rep 38: BSR20181043, 2018.
67. Bhuniya D, Umrani D, Dave B, Salunke D, Kukreja G, Gundu J, Naykodi M, Shaikh NS, Shitole P, Kurhade S, *et al*: Discovery of a potent and selective small molecule hGPR91 antagonist. Bioorg Med Chem Lett 21: 3596-3602, 2011.
68. Velcicky J, Wilcken R, Cotesta S, Janser P, Schlapbach A, Wagner T, Piechon P, Villard F, Bouhelal R, Piller F, *et al*: Discovery and optimization of novel SUCNR1 inhibitors: Design of zwitterionic derivatives with a salt bridge for the improvement of oral exposure. J Med Chem 63: 9856-9875, 2020.